ELSEVIER

Biochimica et Biophysica Acta 1318 (1997) 299–306

BIOCHIMICA ET BIOPHYSICA ACTA
BBA

Proton and electrical charge translocation by cytochrome-*c* oxidase

Mårten Wikström *, Joel E. Morgan, Michael I. Verkhovsky

Helsinki Bioenergetics Group, Department of Medical Chemistry, Institute of Biomedical Sciences and Biocenter Helsinki, P.O. Box 8, FI-00014 University of Helsinki, Helsinki, Finland

Received 2 September 1996; accepted 31 October 1996

Abstract

O_2 is reduced to 2 H_2O in the cytochrome-*c* oxidase reaction. The four protons consumed are taken from the inside (*i* phase) of the inner mitochondrial membrane, whereas the electrons are taken from cytochrome *c* on the opposite side (*o* phase). These electron and proton transfers contribute 50% to the generation of $\Delta\mu_{H^+}$ across the membrane. The other 50% comes from the 4 H^+ that are translocated ('pumped') across the membrane per O_2 reduced. In this paper we assess the number of electrical charges translocated in the different discrete steps of the catalytic cycle, by assessing the linkage of each step with electron transfer, proton uptake/release, and proton pumping. $\Delta\mu_{H^+}$ and pH_i determine the number of protons bound to the enzyme from the *i* phase. At high $\Delta\mu_{H^+}$ these protons may dissociate, so that the number of protons bound to a discrete state of the enzyme may be lower than at $\Delta\mu_{H^+}=0$. This analysis may reconcile the difference between proton uptake stoichiometries previously determined for the isolated enzyme (Mitchell, R. and Rich, P.R. [1994] Biochim. Biophys. Acta 1186, 19–26) with those measured at high $\Delta\mu_{H^+}$ in intact mitochondria (Wikström, M. [1988] Chem. Scr. 28A, 71–74).

Keywords: Cytochrome-*c* oxidase; Electron transfer; Proton transfer

1. Introduction

It is well understood today that electron transfer in the respiratory chain generates an electrochemical proton gradient ($\Delta\mu_{H^+}$), which is the immediate driving force for the oxidative synthesis of ATP, as first proposed in Mitchell's chemiosmotic theory [1]. Today, much research is devoted towards understanding the molecular mechanisms in the enzyme complexes of the respiratory chain that underly the coupling of electron transfer to formation of $\Delta\mu_{H^+}$. In this paper we will analyse this coupling for the cytochrome-*c* oxidase (Complex IV) reaction in the light of the most recent available experimental evidence. We will develop a model of how individual steps in the catalytic cycle contribute to the translocation of electrical charges across the membrane (by electron and proton transfer), and identify where more experimental data will be required to test this model.

2. Overall charge translocation in the cytochrome-*c* oxidase reaction

The final reaction step of cell respiration in eukaryotes and many prokaryotes is the cytochrome-*c* oxidase reaction

$$4e^- + 4H^+ + O_2 \rightarrow 2H_2O \quad (1)$$

where electrons derived from catabolism are donated to cytochrome-*c* oxidase via the respiratory chain,

* Corresponding author. Fax: +358 9 1918296.

PII S0005-2728(96)00152-1

reducing dioxygen to water. Although we will here concentrate on the mitochondrial enzyme, much of the discussion will be directly applicable on the analogous haem-copper oxidases in the cell membrane of many bacteria.

The overall reaction (Eq. (1)) consumes four protons. Due to the location of the enzyme in the inner mitochondrial membrane, and the vectorial nature of the catalytic chemistry (the electrons derive from the outside and the protons from the inside of the membrane), Eq. (1) may instead be written

$$4\,e_o^- + 4\,H_i^+ + O_2 \rightarrow 2\,H_2O \qquad (2)$$

where the indices *o* and *i* refer to the outer and inner side of the membrane, respectively. The asymmetric organization of the catalytic chemistry serves to generate both $\Delta\psi$ and ΔpH across the membrane at a stoichiometry of 4 electrical charges (q) translocated and 4 protons taken up per O_2 reduced.

The site of O_2 reduction is a binuclear haem iron/copper centre (Fe_{a3}; Cu_B), which is located well within the membrane-embedded enzyme protein [2,3], at a depth corresponding to ca. 1/2 of the membrane dielectric [4]. The electron donor to this site is another haem (Fe_a), which is located at about the same depth. Fe_a, in turn, receives electrons from a fourth centre, Cu_A, which is located in a peripheral domain [2,3] outside the membrane dielectric [5]. These locations are schematically depicted in Fig. 1, which also shows the approach of protons from the *i*-side.

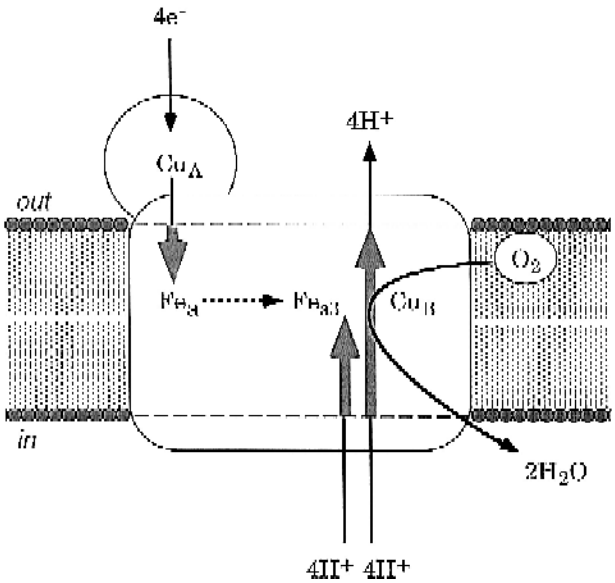

Fig. 1. The electrogenic steps of cytochrome-*c* oxidase catalysis. The enzyme is depicted schematically in the inner mitochondrial membrane. Turnover is coupled to the following electrogenic events (solid arrows): uptake of four electrons from the *o*-phase, net uptake of four protons from the *i*-phase, and translocation of four protons from *i* to *o* by the pump. The dashed lines denote the dielectric barrier.

In addition, and as also shown in Fig. 1, cytochrome-*c* oxidase functions as a proton pump that translocates 4 protons from the *i* to the *o* side per O_2 reduced [6]. This activity doubles the efficiency of energy conservation, and the complete cytochrome-*c* oxidase reaction can be written

$$4\,e_o^- + 8\,H_i^+ + O_2 \rightarrow 2\,H_2O + 4\,H_o^+ \qquad (3)$$

3. Catalysis of O_2 readuction

In the past 10 years the catalytic details of O_2 reduction by cytochrome-*c* oxidase have been intensely studied (for reviews, see Refs. [7–10]). A shorthand scheme of the catalytic cycle is shown in Fig. 2, which serves our present purposes though it lacks much of the detail (note especially that proton-pumping is not shown). The symbols represent states of the binuclear site. Reduction of this site in the oxidized enzyme (state **O**; Fe^{3+}_{a3} Cu^{2+}_B) by 2 electrons leads to the reduced ferrous-cuprous state (**R**), which can react with O_2 to form the primary 'oxy' intermediate (**A**; [11]). If no further electrons are available, **A** is converted to the so-called **P** ('peroxy') state (here called $\mathbf{P_M}$) at a rate of ca. 5000 s^{-1} at room temperature [11–13]. However, if a third electron is already available at Fe_a, then the decay of **A** is much faster (ca. 30 000 s^{-1}; [14–17]), and the primary product is $\mathbf{P_R}$ [18]. We have recently shown that $\mathbf{P_R}$ has the same spectral characteristics as $\mathbf{P_M}$, viz. a sizable absorption peak at 607 nm [18]. The structure of Fe_{a3} (possibly ferric peroxy) is hence almost certainly the same in $\mathbf{P_R}$ as in $\mathbf{P_M}$, although there is one more electron in the binuclear centre in the former case. This 'extra electron' is probably on Cu_B, which would then be cupric in $\mathbf{P_M}$ and cuprous in $\mathbf{P_R}$ [18].

Whilst $\mathbf{P_M}$ is relatively stable in the absence of an electron donor, $\mathbf{P_R}$ converts rapidly (ca. 5000 s^{-1}) to the **F** (ferryl) intermediate [19–22] with the characteristic absorption maximum near 580 nm [18]. Finally, the fourth electron reduces the **F** intermediate back to

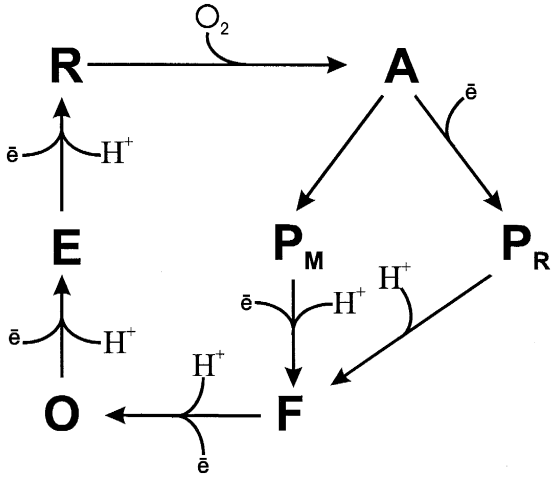

Fig. 2. Simplified scheme of the catalytic cycle of cytochrome-*c* oxidase. The symbols denote the state of the binuclear haem iron-copper centre. **O** (ferric/cupric) receives one electron to form the one-electron-reduced state (**E**). Uptake of a second electron leads to the reduced state (**R**; ferrous/cuprous), which can react with O_2 to form the 'oxy' intermediate (**A**; ferrous-oxy/cuprous). If no further electrons are available, **A** decays into the 'peroxy' state $\mathbf{P_M}$, which may be converted to the oxyferryl state **F** by uptake of a third electron. If the third electron is already available when O_2 binds, it is rapidly transferred to the binuclear site to form the 'peroxy' state $\mathbf{P_R}$, which subsequently decays to the **F** state. The fourth electron reduces **F** back into the **O** state. The proton uptake steps shown are those observed for the isolated detergent-solubilized enzyme. Note that proton-pumping is not included in this scheme.

the **O** state, and the cycle is completed. A ferric haem iron-hydroxy intermediate has been identified in this last step [21] (not shown). We have recently confirmed by discrete photoinjection of one electron into the $\mathbf{P_M}$ and **F** states of the enzyme that the $\mathbf{P_M}$ state is one electron equivalent more oxidized overall than **F**, and two equivalents more oxidized than the **O** state [23].

4. Tracing the protons taken up during catalysis

Fig. 2 also summarizes the net proton uptake that is linked to the various steps of the catalytic cycle. This information has largely been contributed by the work of Rich and collaborators on the isolated detergent-solubilized enzyme [24,25]. Briefly, two protons are taken up on the two-electron reduction of the binuclear site. These must be taken up from the *i*-side, although this has never been shown directly. However, if they were taken from the *o*-side, then reduction of the binuclear centre would not be electrogenic (cf. Fig. 1), which is inconsistent with the finding that the apparent E_m values of the binuclear site metals are sensitive to $\Delta\psi$ [26,27]. Upon O_2 binding and subsequent formation of $\mathbf{P_M}$ there is no net protonic change. This is an important finding (cf. below), showing that the two protons that were taken up on reduction remain bound to the enzyme, although we cannot be certain at this time *how* they are bound, nor whether they are bound differently in the **R** and **P** states. Oliveberg et al. [28], who time-resolved the protonations involved in the reaction of the fully reduced solubilized enzyme with O_2, showed that there was also no net proton uptake associated with the 30 000 s^{-1} phase in which $\mathbf{P_R}$ is formed, but that an equal amount of protons were taken up corresponding roughly to the $\mathbf{P_R} \rightarrow \mathbf{F}$ and $\mathbf{F} \rightarrow \mathbf{O}$ conversions. We can hence conclude that the $\mathbf{A} \rightarrow \mathbf{P}$ step is not linked to net proton uptake whether the product is $\mathbf{P_M}$ or $\mathbf{P_R}$. In agreement with Oliveberg et al. [28], Rich et al. [24,25] showed that the $\mathbf{P} \rightarrow \mathbf{F}$ and $\mathbf{F} \rightarrow \mathbf{O}$ steps are each associated with the net uptake of one proton.

5. Partial reversal of the oxygen reaction

Wikström [29] showed that some of the catalytic events of the enzyme (Fig. 2) could be partially reversed. When a high $\Delta\mu_{H^+}$ was applied to mitochondria as a result of ATP hydrolysis, and a high electron acceptor potential (E_h) was simultaneously applied at cytochrome *c*, the oxidized enzyme (**O** state) was converted into **F**, and into **P**, but not further. Wikström and Morgan [30] confirmed kinetically that both these transitions are associated with the transfer of one electron from the binuclear site to ferricytochrome *c*. The **P** state formed in this reaction is hence $\mathbf{P_M}$. With this technique, an equilibrium is established between the $\Delta\mu_{H^+}$ (or $ATP/ADP \cdot P_i$) and the $\mathbf{P}/\mathbf{F}$ and $\mathbf{F}/\mathbf{O}$ couples, respectively, and the equilibrium properties may be studied. The necessary mechanistic linkage to achieve such equilibria is that both the proton-translocating ATP synthase and these partial reaction steps of the oxidase are coupled to proton and electrical charge translocation across the membrane (Eq. (3)).

Titrations of the **P/F** and **F/O** equilibria with phosphorylation potential ($ATP/ADP \cdot P_i$) revealed that the **P → F** and **F → O** steps are linked to the synthesis of 0.9–1.0 and 0.70–0.75 ATP molecules, respectively [31]. The overall ATP/O_2 ratio of the oxidase reaction is 2.0 ($P/O = 1$; [32]). From this follows that these reaction steps must together include most (80–88%) of the $\Delta\mu_{H^+}$-generating steps in the catalytic cycle. Since proton pumping accounts for 50% of the overall charge translocation (compare Eqs. (2) and (3)), it is clear that at least the major energy-requiring steps of proton pumping must be associated with the **P → F** and **F → O** steps (not shown in Fig. 2). Note here that most of the energy requirement of 'proton-pumping' comes from the translocation of electrical charge across the dielectric; the actual uptake and/or release of protons from/into the aqueous phases on the two sides of the membrane is expected to be associated with a much smaller energy requirement.

The finding that the oxidative phase of the cytochrome oxidase reaction (**R → O**; Fig. 2) provides the major linkage to energy conservation nicely confirms the proposal by Muraoka and Slater [33] that it is 'the reaction between reduced cytochrome a_3 and O_2 that is coupled to ATP synthesis'. However, this leads to an apparent dilemma: reduction of the binuclear site (**O → R**) is coupled to translocation of 2q across the membrane ($2e^-$ and $2H^+$ across 1/2 the dielectric; see above), which corresponds to 25% of the 8q translocated in the complete reaction. How, then, could the **P → O** steps contribute more than 80%? We will attempt to answer this question below.

6. Proton uptake coupled to the P → F and F → O transitions

Wikström [34] titrated the **P → F** and **F → O** equilibria with pH in mitochondria supplemented with nigericin ($pH_o = pH_i$), at constant high $\Delta\mu_{H^+}$ and E_h. The former step was, apparently, associated with net uptake of 2 H_i^+, and the latter with either 0 (at $pH > 7.2$) or 2 H_i^+ ($pH < 7.2$), i.e., ~1 proton at pH ~ 7. As pointed out by Peter Rich and his associates [24,25], this is inconsistent with their finding that only one proton is taken up in both these steps in the solubilized enzyme (i.e., at $\Delta\mu_{H^+} = 0$), and that the latter stoichiometries (Fig. 2) were found to be pH-independent in the pH 7.2–8.5 range. We now turn to address this discrepancy first. As already suggested by Mitchell and Rich [25], we also anticipate that it may be due to the vastly different conditions at high and low $\Delta\mu_{H^+}$.

Assuming that hydrolysis of 1 ATP in mitochondria is associated with the translocation of 4 H^+, the linkage of the **P → F** and **F → O** steps to ATP synthesis (see above) would mean that these steps are associated with translocation of approx. 4 and 3 protons (or equivalent electrical charges; Δq), respectively [31]. Let us now try to trace how this might be achieved.

In the backward transition from the **O** state into the **F** state, one electron is transferred from the

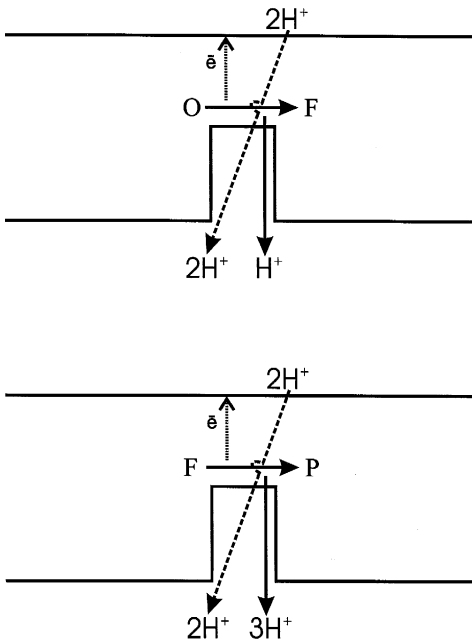

Fig. 3. Electrical charge translocation during reversal of the catalytic reaction at high $\Delta\mu_{H^+}$. The upper scheme depicts the electron and proton transfer steps associated with the transition from the **O** state to the **F** state, relative to the dielectric barrier in the membrane-embedded protein. The lower scheme shows the corresponding reactions associated with the **F** to **P** ($\mathbf{P_M}$) transition. Reversal of the proton pumping step is shown by the dashed arrow with 2 H^+. A proton 'well' is depicted to traverse about half way across the dielectric barrier, connecting the pump and the binuclear site with the aqueous *i* phase (below). Solid arrows with H^+ show deprotonation reactions towards the *i* phase associated with the reaction step; the actual number of these released protons can vary depending on pH (see text).

binuclear centre to cytochrome *c*, which is equivalent to translocation of 0.5 electrical charges across the membrane (0.5 Δq). According to Rich et al. [24,25], this step should also be linked to the release of one proton into the *i* phase (0.5 Δq). As explained above, the **P** → **O** steps are coupled to the major energetic events of proton translocation, half of which is likely to occur at **F** → **O**, i.e., 2 protons translocated (2.0 Δq), as shown in Fig. 3 (upper scheme). Altogether, this yields 3 Δq for this step, in good agreement with the results of titration with phosphorylation potential [31].

In the further conversion of **F** into **P**, the same events as above are expected to occur, i.e., 1 e^- (0.5 Δq), one H^+ released to the *i* side (0.5 Δq), as found by Rich et al. [24,25], and 2 H^+ translocated by the pump (2 Δq), again yielding a total of 3 Δq. Yet, the ATP/ADP · Pi titrations suggested 4 Δq for this step [31].

At this point we should stress that when protons are taken up into the enzyme from the *i* side upon reduction, they presumably cross ca. 1/2 of the dielectric barrier to largely neutralize the electrons taken up. This is sometimes described as a proton 'well' [35] connecting the interior membrane-embedded domain of the protein with the aqueous phase on the *i* side of the membrane. The local proton activity ('local pH') near the proton-binding group at the bottom of such a well will then not only depend on pH_i, but also on $\Delta\psi$ across the well, i.e., ca. one half of the membrane potential, so that

$$pH_{loc} \sim pH_i + \Delta\psi[mV]/120 \quad (4)$$

where pH_{loc} describes the proton activity at the bottom of the well, pH_i is the pH in the aqueous *i* phase, and $\Delta\psi$ (in mV) is the transmembrane potential [34].

This means that when mitochondria experience a high $\Delta\mu_{H^+}$ (e.g., due to ATP hydrolysis), this has the effect of elevating pH_{loc} near internal proton binding groups to an extent that may, in experimental practice, be very difficult to achieve with the detergent-solubilized enzyme at $\Delta\mu_{H^+} = 0$, and that may well approach or exceed the pK_a of that group. Such an acid/base group would in these circumstances tend to dissociate its proton through the 'well' into the aqueous *i* phase. This proton dissociation would be difficult to study in the isolated enzyme, because suspending the enzyme in a solution of very high pH is likely to destroy its structure. It follows directly from this that less protons may be associated with various states of the enzyme at high $\Delta\mu_{H^+}$ than at $\Delta\mu_{H^+} = 0$ (solubilized enzyme).

Now recall that the **P** state of the solubilized enzyme retains the two protons that were taken up on reduction of the binuclear site (Fig. 2; [24,25]). We do not know how they are bound, but since they were taken up from the *i* side, it seems reasonable to assume that they may be accessible from that side of the membrane. Under the influence of the high $\Delta\mu_{H^+}$, the **P** state might therefore release both these protons into the *i*-phase, which would be equivalent to one additional Δq, as depicted in Fig. 3 (lower scheme). This would increase the total Δq associated with the **F** → **P** step to 4, which would explain the observed linkage of the **P** → **F** step to translocation of 4 charges (i.e., hydrolysis of 1 ATP). The entire **P** → **O** transition would therefore be associated with translocation of 7q, i.e., 87.5% of the charge translocation in an entire turnover. Note, however, that this calculation is based on experiments on *the reverse reaction*, and that the reaction in the forward direction might take a somewhat different course (see below).

Based on the above, we predict that the **P**-> **F**

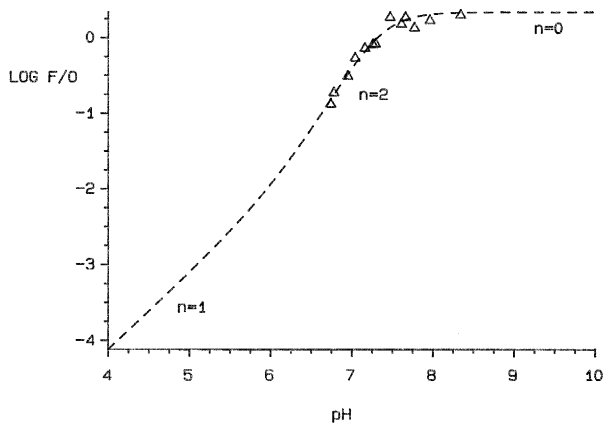

Fig. 4. pH-dependence of the **P**/**F** equilibrium at high $\Delta\mu_{H^+}$. The experimental data points are from Fig. 2B in Ref. [34]. The dashed line shows the best fit for a model where the **P(0)** states converts either into **F(3)** or **F(2)**, with an apparent pK_a of 6.3 for dissociation of **F(3)**. The numbers in parentheses denote the number of bound mobile protons. Simulation software, GIM (Graphic Interactive Management; Alexander Drachev, Tempe, Arizona). The *n*-values indicate the pH domains in which *n* protons are involved in the **P**/**F** conversion.

step may be associated with *net* uptake of *three* protons at high $\Delta\mu_{H^+}$ (Fig. 3B), instead of 1 as found at $\Delta\mu_{H^+}=0$ [24,25]. However, Wikström [34] reported a 2 H^+ dependence, which led us to reinvestigate the earlier data on the pH-dependence of this step. According to Rich et al. [24,25], the **F** state has taken up a total of 3 protons at $\Delta\mu_{H^+}=0$ (Fig. 2; whether some of these form water does not matter in this context). By analogy to the proposed deprotonation of the **P** state above, we postulate that (at least) one of these protons in **F** can be driven into the aqueous *i* phase at high $\Delta\mu_{H^+}$, giving rise to an **F** state with 2 bound protons, but with unchanged spectral characteristics. At high $\Delta\mu_{H^+}$ the **P->F** step could therefore be associated with uptake of *either* two *or* three protons depending on the pH_{loc} relative to the pK_a of the protonatable group in **F**. Fig. 4 shows the data points from Ref. [34] and the best fit to this particular model, which yields an *apparent* pK_a value of 6.30 ($\pm$0.43 S.D.) for dissociation of the proton from the **F** state (the model is shown schematically in Fig. 6 below). Fig. 4 clearly calls for more data at lower pH to test this possibility further, but the available data are not inconsistent with the model.

At high $\Delta\mu_{H^+}$ the **F/O** transition was found, apparently, to be coupled to uptake/release of 2 H^+ below pH 7.2 and to 0 H^+ at higher pH [34]. The maximum number of protons that can be taken up by the enzyme in the **O** state should be 4 (since 2 H_2O molecules are finally produced from one O_2). The slope of zero suggests, therefore, that at high pH and $\Delta\mu_{H^+}$ the **O** state may dissociate two of these protons. Fig. 5 shows that the fit of the pH titration data with such a model is reasonable, but that more data would again be necessary to test this and to assess the precise *p*K values.

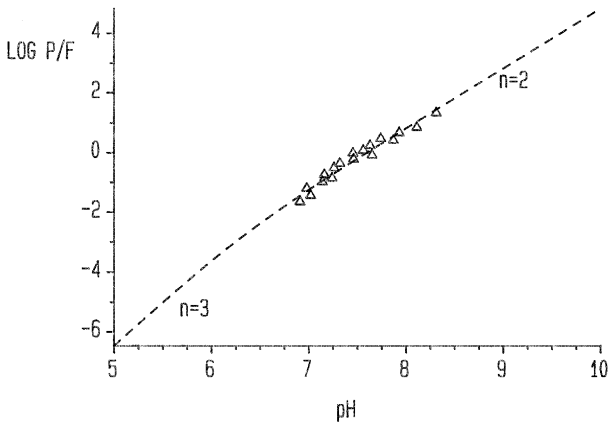

Fig. 5. pH-dependence of the **F/O** equilibrium at high $\Delta\mu_{H^+}$. Experimental data points are from Fig. 2A in Ref. [34]. The dashed line shows the best fit to a model where the apparent pK_a is 6.3 for dissociation of **F(3)**, and 6.4 and 8.3 for dissociation of **O(4)** and **O(3)**, respectively. See also legend for Fig. 4.

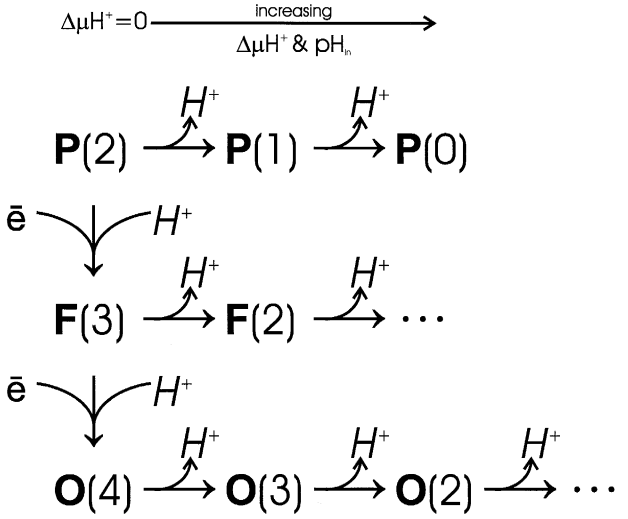

Fig. 6. Scheme of the different protonation states of the **P**, **F** and **O** intermediates. The number of bound 'mobile' protons is shown in parentheses for each state. At low $\Delta\mu_{H^+}$ only the left column of states (**P(2)**, **F(3)** and **O(4)**) is easily accessible experimentally.

Fig. 6 provides a shorthand summary of our tentative proposal for the protonic connectivity between the **P**, **F** and **O** states. The **O** state of the solubilized enzyme (i.e., at $\Delta\mu_{H^+}=0$) is depicted to 'contain' 4 protons. These are the protons of the two water molecules formed when the four-electron reduced enzyme reacts with O_2. When **O** is oxidized into **F** and further into **P** under the influence of $\Delta\mu_{H^+}$, these two water molecules will eventually form bound peroxide (in **P**), and protons will be drawn into the *i* phase. Hence, they are 'labile', and the acidic **O** state may be denoted **O(4)**. On the other hand, upon reduction of the **O** state to **R**, the enzyme takes up two electrons (not shown in Fig. 6) whereby these four protons leave in the form of two water molecules, and two 'new' protons are taken up (Figs. 1 and 2).

Summarizing, **P** has two bound protons at $\Delta\mu_{H^+}=0$ [**P(2)**]; its reduction to **F(3)** and to **O(4)** in such circumstances is associated with uptake of one proton in each step (Fig. 6; left column), in accordance with

the observations of Rich et al. [24,25]. When $\Delta\mu_{H^+}$ is increased, however, less protonated states of all three intermediates become experimentally accessible. In such conditions the apparent pK_a values of their interconversion can be uniquely observed in pH titrations. Both protons of the **P** state are apparently easily lost in such conditions (see above). The **P** to **F** transition will thus be associated with the uptake of either two or three protons (Fig. 4), depending on pH_i relative to the apparent pK_a of the **F(3)** state, which is estimated to be of the order of 6–6.5. In the transition from **F** to **O** three protonic **O** states may be encountered (Fig. 6), and this transition may show a change of slope between 0 and 2 H^+ per pH unit (Fig. 5). The data published are for a too limited pH range to make any firm quantitative conclusions about the pK_a values involved. Nevertheless, the scheme of Fig. 6 is consistent with the published data, and can explain the apparent inconsistency between proton uptake stoichiometries determined for the isolated enzyme [24,25], relative to the mitochondrial enzyme at high $\Delta\mu_{H^+}$ [34].

The structural counterparts of the different protonation states in Fig. 6 are not yet understood. As an example, however, the binuclear site metals in the **O(2)** state could correspond to [Fe^{3+}-OH^- Cu^{2+}-OH^-] or [Fe^{3+}-O^{2-}-Cu^{2+}] structures, which after uptake of one and two protons might form [Fe^{3+} Cu^{2+}-OH^-] and [Fe^{3+} Cu^{2+}], respectively, corresponding to the **O(3)** and **O(4)** states. We emphasize, however, that the protons need not necessarily be bound to the binuclear site metal ligands.

7. Charge translocation in the forward reaction

As concluded above (Fig. 2), when the fully reduced enzyme reacts with O_2 at $\Delta\mu_{H^+} = 0$, a third electron is already in the binuclear site when the **P** state ($\mathbf{P_R}$) is formed from **A**. In contrast, the $\mathbf{P_M}$ state has one less electron, and this is the form of **P** generated both when the mixed-valence enzyme reacts with O_2, and as a result of ATP-linked reversal of the catalytic events. This difference readily accounts for the aforementioned discrepancy regarding the very high degree of linkage of the $\mathbf{P} \rightarrow \mathbf{O}$ step to translocation of charge, as determined from the reversed reaction:

At low $\Delta\mu_{H^+}$, 2q are translocated on reduction of the binuclear site ($2e^- + 2\ H^+$ taken up; Fig. 2), and a further 0.5 q is translocated when the third electron reaches Fe_a and the binuclear site. O_2 binding leads eventually to formation of $\mathbf{P_R}$, and this step is not associated with translocation of charge, as we have recently shown by direct time-resolved electrometric monitoring of cytochrome oxidase vesicles [36]. Then follows the $\mathbf{P_R} \rightarrow \mathbf{F}$ step, which is associated with net uptake of 1 H^+ (0.5 Δq) and translocation of 2 H^+ (2 Δq). At about the same time the fourth electron is redistributed between Cu_A and Fe_a leading to about half-reduction of the latter (0.25 Δq). Thus the total charge translocated in this step is ca. 2.75 Δq. The events associated to the subsequent $\mathbf{F} \rightarrow \mathbf{O}$ step are expected to be energetically almost exactly the same (2.75 Δq), as also confirmed by the generation of an equal extent of $\Delta\psi$ in this step [36]; the remaining 0.5 electron at Cu_A (and 0.5 at Fe_a) flows to the binuclear site, yielding 0.25 Δq due to electron translocation.

In the forward direction, therefore, the $\mathbf{P_R} \rightarrow \mathbf{O}$ transition is linked to translocation of a total of 5.5 Δq, which together with the 2.5 Δq translocated during reduction of the enzyme yields the total of 8 Δq (Eq. (3)). Here, the reaction steps of the $\mathbf{P} \rightarrow \mathbf{O}$ transition only contribute some 69% to the total charge translocation, enzyme reduction contributing 31%. This differs from the number of charges translocated when the **O** state is driven backwards into $\mathbf{P_M}$ by ATP hydrolysis, which is coupled to 7 Δq (Fig. 3; see above). Clearly, the precise contributions to Δq of the reductive and oxidative parts of the catalytic cycle can vary, depending on the energy state of the mitochondrion. At high $\Delta\mu_{H^+}$ (State 4 mitochondria) it is quite possible that O_2 reacts predominantly with the mixed-valence enzyme ($2e^-$), because electron transfer from cytochrome *c* to Fe_a will be disfavoured by $\Delta\psi$. In this case only 2q might be translocated during enzyme reduction (25%; uptake of $2e^-$ and 2 H^+). O_2 binding will result in the $\mathbf{P_M}$ state, and the $\mathbf{P_M} \rightarrow \mathbf{O}$ transition will be associated with uptake of both the third and fourth electrons, and translocation of 6q. However, proton uptake on reduction of the enzyme might also be decreased at high $\Delta\mu_{H^+}$ (cf. the deprotonation of the **P(2)**, **F(3)** and **O(4)** states discussed above); hence the contribution of the reduction phase to overall Δq

might be decreased even further, to the minimum of 1 Δq (12.5%) due to electron uptake alone.

We conclude that the relative contribution of the oxidative **P** → **O** steps of the catalytic cycle to energy conservation, relative to that of the reductive **O** → **R** steps, will be maximal (87.5%) at high $\Delta\mu_{H^+}$ and minimal (68.8%) at $\Delta\mu_{H^+} = 0$.

An interesting case may be the one reported by Zaslavsky et al. [37], who photoinjected an electron into the **F** state of cytochrome oxidase in vesicles (the **F** was formed by addition of H_2O_2 to the oxidized enzyme), and monitored Δq by direct electrometry. They found that if the observed **F** → **O** transition is *assumed* to be coupled to net uptake of 1 H^+ (Fig. 2; [20,21]), then the Δq due to proton pumping would be only 1.5 and not 2.0, in contrast to the conclusions in Ref. [27]. Zaslavsky et al. [37] discussed two possible explanations for underestimating this value. However, a third possible rationalization is that they were, in fact, monitoring the transition from **F(2)** to **O(2)** (Fig. 7 in Ref. [37]) due to the high pH (pH 8) in their experiment, and the $\Delta\mu_{H^+}$ generated by the reaction. If so, there may have been no *net* proton uptake associated with this transition, and then the number of pumped protons would amount to the predicted 2.0 for this step.

Acknowledgements

This work was supported by grants from the Jusèlius Foundation, the Academy of Finland and Biocentrum Helsinki. We thank Ms. Satu Sankkila for secretarial assistance.

References

[1] Mitchell, P. (1976) J. Theor. Biol. 62, 327–367.
[2] Iwata, S., Ostermeier, C., Ludwig, B. and Michel, H. (1995) Nature 376, 660–669.
[3] Tsukihara, T., Aoyama, H., Yamashita, E., Tomizaki, T., Yamaguchi, H., Shinzawa-Itoh, K., Nakashima, R., Yaono, R. and Yoshikawa, S. (1995) Science 269, 1069–1074.
[4] Hinkle, P. and Mitchell, P. (1970) Bioenergetics 1, 45–60.
[5] Rich, P.R., West, I.C. and Mitchell, P. (1988) FEBS Lett. 233, 25–30.
[6] Wikström, M. (1977) Nature 266, 271–273.
[7] Babcock, G.T. and Wikström, M. (1992) Nature 356, 301–309.
[8] Malmström, B.G. (1993) Acc. Chem. Res. 26, 332–338.
[9] Einarsdottir, O. (1995) Biochim. Biophys. Acta 1229, 129–147.
[10] Ferguson-Miller, S. and Babcock, G.T. (1996) Chem. Revs., in press.
[11] Chance, B., Saronio, C., and Leigh, J.S., Jr. (1975) J. Biol. Chem. 250, 9226–9237.
[12] Hill, B.C. and Greenwood, C. (1983) Biochem. J. 215, 659–667.
[13] Han, S., Ching, Y.C. and Rousseau, D.L. (1990) J. Am. Chem. Soc. 112, 9445–9451.
[14] Hill, B.C. and Greenwood, C. (1984) Biochem. J. 218, 913–921.
[15] Han, S., Ching, Y.C. and Rousseau, D.L. (1990) Proc. Natl. Acad. Sci. USA 87, 2491–2495.
[16] Hill, B.C. (1994) J. Biol. Chem. 269, 2419–2425.
[17] Verkhovsky, M.I., Morgan, J.E. and Wikström, M. (1994) Biochemistry 33, 3079–3086.
[18] Morgan, J.E., Verkhovsky, M.I. and Wikström, M. (1996) Biochemistry, in press.
[19] Orii, Y. (1988) Ann. N.Y. Acad. Sci. 550, 105–117.
[20] Varotsis, C. and Babcock, G.T. (1990) Biochemistry 29, 7357–7362.
[21] Han, S., Ching, Y.C. and Rousseau, D.L. (1990) Nature 348, 89–90.
[22] Ogura, T., Takahashi, S., Hirota, S., Shinzawa-Itoh, K., Yoshikawa, S., Appleman, E.H. and Kitagawa, T. (1993) J. Am. Chem. Soc. 115, 8527–8536.
[23] Verkhovsky, M.I., Morgan, J.E. and Wikström, M. (1996) Proc. Natl. Acad. Sci. USA, in press.
[24] Mitchell, R., Mitchell, P. and Rich, P.R. (1992) Biochim. Biophys. Acta 1101, 188–191.
[25] Mitchell, R. and Rich, P.R. (1994) Biochim. Biophys. Acta 1186, 19–26.
[26] Wilson, D.F. and Dutton, P.L. (1970) Arch. Biochem. Biophys. 136, 583–584.
[27] Rich, P.R. (1988) Ann. N.Y. Acad. Sci. 550, 254–259.
[28] Oliveberg, M., Hallén, S. and Nilsson, T. (1991) Biochemistry 30, 436–440.
[29] Wikström, M. (1981) Proc. Natl. Acad. Sci. USA 78, 4051–4054.
[30] Wikström, M. and Morgan, J.E. (1992) J. Biol. Chem. 267, 10266–10273.
[31] Wikström, M. (1989) Nature 338, 776–778.
[32] Chamalaun, R.A.F.M. and Tager, J.M. (1969) Biochim. Biophys. Acta 180, 204–206.
[33] Muraoka, S. and Slater, E.C. (1969) Biochim. Biophys. Acta 180, 227–236.
[34] Wikström, M. (1988) Chem. Scr. 28A, 71–74.
[35] Mitchell, P. (1968) Chemiosmotic Coupling and Energy Transduction, Glynn Research Ltd., Bodmin, Cornwall, UK.
[36] Verkhovsky, M.I., Morgan, J.E., Verkhovskaya, M.L. and Wikström, M. (1997) Biochim. Biophys. Acta 1318, 6–10.
[37] Zaslavsky, D., Kaulen, A.D., Smirnova, I.A., Vygodina, T. and Konstantinov, A.A. (1993) FEBS Lett. 336, 389–393.